# Supplementary material

# Application of Physiologically-based Pharmacokinetic Modeling for the Prediction of a Drug-drug Interaction between a Combined P-gp and Strong CYP3A inducer and Apixaban and Rivaroxaban

Yukio Otsuka[1], Mary P. Choules[2], Peter L. Bonate[2], Kanji Komatsu[1]

[1] Clinical Pharmacology and Exploratory Development, Astellas Pharma Inc., Tokyo, Japan

[2] Clinical Pharmacology and Exploratory Development, Astellas Pharma Global Development Inc., IL, USA

## S1 Apixaban PBPK Model Development and Verification as a CYP3A4 and P-gp Substrate

### S1.1 Objective

To develop and verify a PBPK model of apixaban for its intended use in a CYP3A and P-gp mediated drug-drug interaction simulation.

### S1.2 Summary

The apixaban PBPK model was developed based on *in vitro*, *in vivo*, and *in silico* data obtained from public domain. At first, a model for intravenous (iv) administration was developed. Then, the iv model was modified by adding an oral (po) absorption component. The model was developed with Advanced Dissolution, Absorption and Metabolism (ADAM) and full PBPK with a permeability limited liver model. The developed model was verified with clinical DDI study results from CYP3A and P-gp inhibitors. The clinical PK and DDI studies used for model development and verification are summarized in Table S1-1 and overall workflow is shown in Figure S1-1.

**Table S1-1 Summary of the Literatures Used in Apixaban Model Development and Verification**

| Data category | Usage | Ref. |
|---|---|---|
| Single dose iv PK at 20 mg | Development | 1 |
| DDI with rifampicin (iv) | Development | 1 |
| Single dose po PK | Development | 1, 2, 3 |
| Multiple dose po PK | Verification | 4 |
| DDI with ketoconazole | Verification | 3 |
| DDI with diltiazem | Verification | 3 |
| DDI with cyclosporin | Verification | 5 |

**Figure S1-1 Overall Workflow of Apixaban PBPK Model Development and Verification**

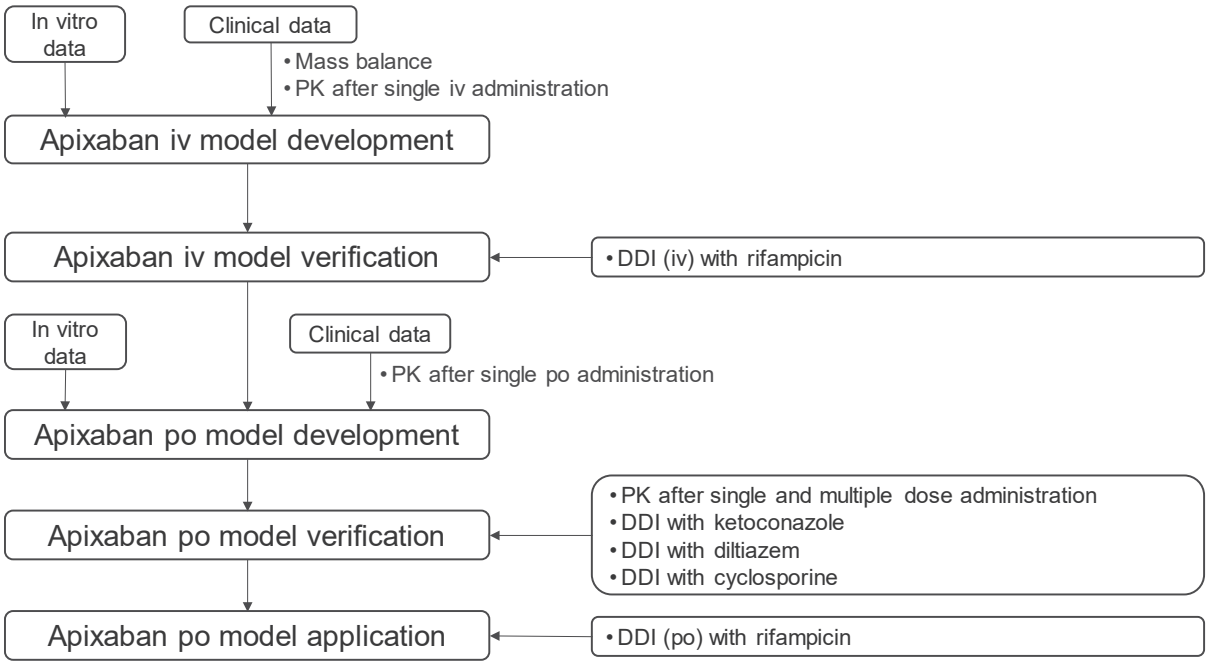


In a human mass balance study, 24.5% (unchanged drug; 21.5%) and 56% (unchanged drug; 34%) of dosed radioactivity was recovered in urine and feces, respectively, after oral [$^{14}$C]apixaban administration[6]. The total recovery of dosed radioactivity was 80.5%; thus, an unrecovered 19.5% was assigned to an unknown elimination pathway. As apixaban is considered a low-permeable compound[7], unchanged drug excreted in feces is considered the nonabsorbed portion. Hence, 66% of orally administered apixaban was assumed to be absorbed from gut and have low first-pass metabolism; bioavailability was 66%. This assumption is valid since the reported absolute bioavailability ranged from 49% to 86%[8]. For the hepatic metabolism, CYP3A is considered to take major contribution with minor contribution of other CYP isoforms[9]. However, DDI study results suggested a low contribution of CYP3A in liver (See details in Section S1.3). Further, the metabolite mainly detected in feces (*O*-demethylapixaban) was generated with recombinant human CYP1A2[10]. Taken together, the contribution of CYP3A4 on hepatic metabolism was optimized using clinical DDI results with rifampicin. Elimination pathway and mass balance assumptions are shown in Figure S1-2.

**Figure S1-2 Elimination Pathway and Mass Balance of Apixaban after Oral Administration**

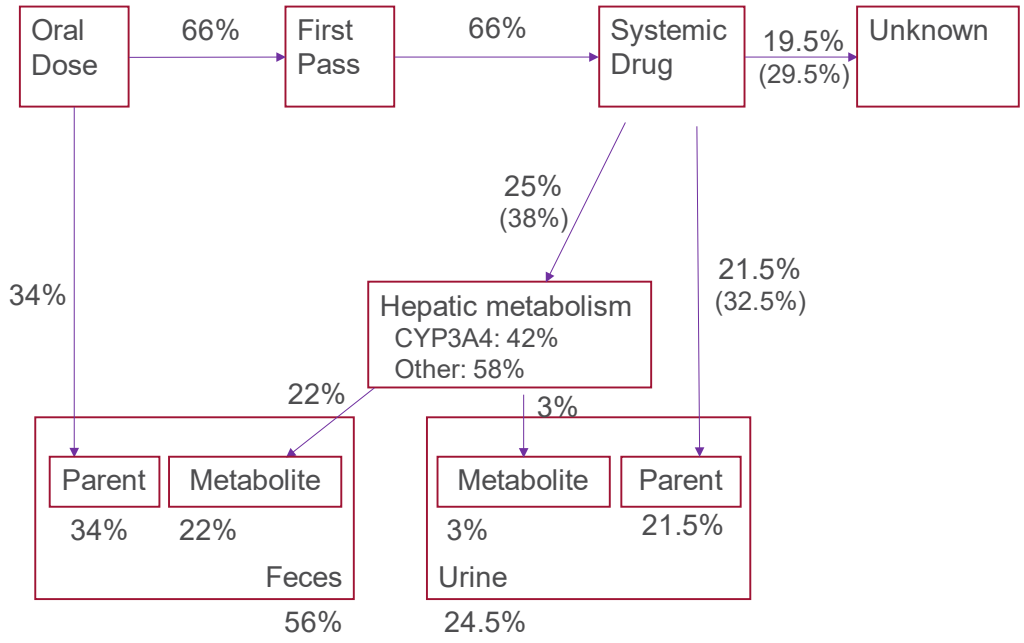


The values in parenthesis are correction for iv administration

## S1.3 Apixaban PBPK model development

In the iv model development, clinically observed systemic clearance after iv administration ($CL_{iv}$) was used for the calculation of CYP3A4 intrinsic clearance ($CL_{int,CYP3A4}$) in liver. The unknown elimination was assigned to additional systemic clearance accounted for 0.974 L/h. Renal clearance ($CL_r$) was calculated to be 1.07 L/h from $CL_{iv}$ (3.3 L/h)[9] and corrected excretion ratio of unchanged drug into urine after iv administration (32.5%). When glomerular filtration ratio (GFR) and body surface area (BSA) were assumed to be 130 mL/min/1.73m$^2$ and 1.94 m$^2$, respectively, filtration clearance was calculated as 0.88 L/h. The calculated filtration clearance indicates filtration accounts for the largest part of renal clearance. Accordingly, P-gp mediated secretion clearance in the kidney was not considered in the current modeling.

Volume of distribution at steady-state ($V_{ss}$) was predicted with Simcyp built-in method 2 which was originally reported by Rodgers and Rowland[11]. The calculated $V_{ss}$ agreed with observed data (0.31 L/kg vs 0.27 L/kg for predicted vs observed)[1]. As an initial assumption, 100% contribution of CYP3A4 on hepatic metabolism was tested for the DDI simulation with rifampicin. When 600 mg multiple oral dose rifampicin was concomitantly administered with 5 mg of iv dose apixaban, the extent of DDI was overpredicted (AUC ratio: 0.43 vs 0.61 for predicted vs observed). Thus, the contribution of CYP3A4 was optimized to reproduce observed DDI results with rifampicin. A contribution of 42% of CYP3A4 agreed with the observed data. With the developed iv model, the simulated plasma concentration-time profile (Figure S1-3) and parameters (Table S1-2) reproduced the observed data.

**Figure S1-3 Simulated and Observed Plasma Concentration-time Profile after Single Intravenous Administration of 5 mg of Apixaban**

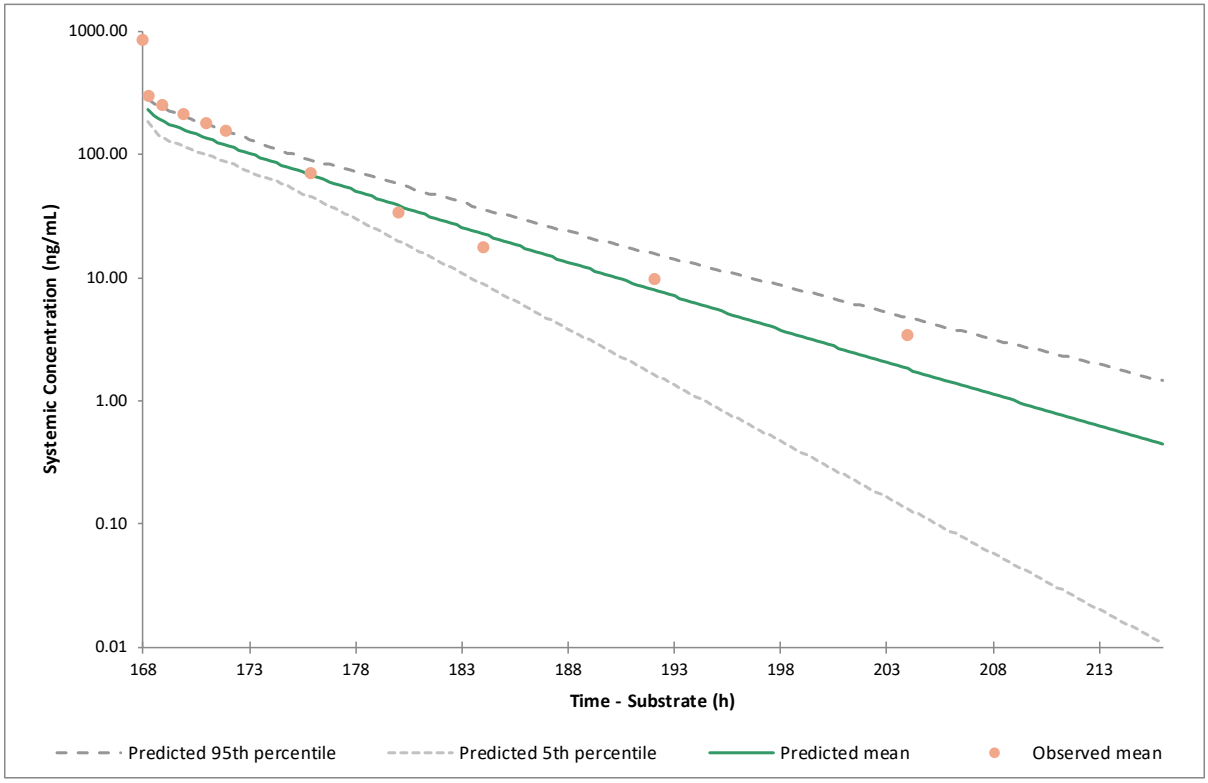


**Table S1-2 Simulated and Observed PK Parameters after Single Intravenous Administration of 5 mg of Apixaban**

| | Observed[1] | Predicted | P/O ratio[†] |
|---|---|---|---|
| **$AUC_t$ (ng·h/mL)** | 1787 (25) | 1539 (17) | 0.86 |
| **$AUC_{inf}$ (ng·h/mL)** | 1816 (25) | 1542 (17) | 0.85 |

Data are expressed as geometric mean (CV%)

[†]: Predicted/Observed ratio

The results of the DDI simulation of oral rifampicin coadministered with iv apixaban after optimization of liver CYP3A4 contribution are shown in Table S1-3.

**Table S1-3 Simulated and Observed PK Parameters after Single Intravenous Administration of 5 mg of Apixaban in Presence of Rifampicin**

| | Observed[1] | Simulated | P/O ratio[†] |
|---|---|---|---|
| **$AUC_t$ (ng·h/mL)** | 1097 (32) | 928 (29) | 0.85 |
| **$AUC_t$ ratio** | 0.61 (0.59-0.64) | 0.60 (0.58-0.63) | 0.98 |

Data are expressed as geometric mean (CV%) for $AUC_t$ and geometric mean ratio (90%CI) for $AUC_t$ ratio

[†]: Predicted/Observed ratio

Next, the apixaban iv model was converted to an oral model by adding oral absorption components. An oral solution was selected as the formulation since oral administration of tablet and solution formulations showed comparable pharmacokinetic properties in a clinical study[12]. $P_{eff,man}$ was predicted from $P_{app}$ in LLC-PK1 cells[13] with Simcyp simulator's built-in model. When apixaban was administered to distal small bowel or ascending colon, the exposure of apixaban decreased by approximately 60% and 84%, respectively, compared to oral administration indicating region-dependent apparent permeability[7]. In order to take into account the regional difference in apparent permeability, $P_{eff,man}$ of ileum IV and colon were reduced by 60% and 84%, respectively. Further, intrinsic clearance for P-gp ($CL_{int,P\text{-}gp}$) in intestine was estimated from *in vitro* P-gp facilitated transport velocity data[13]. Finally, P-gp activity was adjusted to better reproduce observed $C_{max}$ and $AUC_{inf}$ by modifying relative activity factor/relative expression factor (RAF/REF) of intestinal P-gp based on sensitivity analysis. The results of sensitivity analysis and observed and simulated plasma concentration-time profile are shown in Figure S1-4. A scalar of 25 was used to reproduce observed clinical absorption data. The parameters of final apixaban model are summarized in Table S1-4.

**Figure S1-4 Sensitivity Analysis of Scaling Factor of Intestinal P-gp on Plasma Exposure of Apixaban (A) and Simulated and Observed Plasma Concentration-time Profile after Single Oral Administration of 10 mg of Apixaban (B)**

(A)

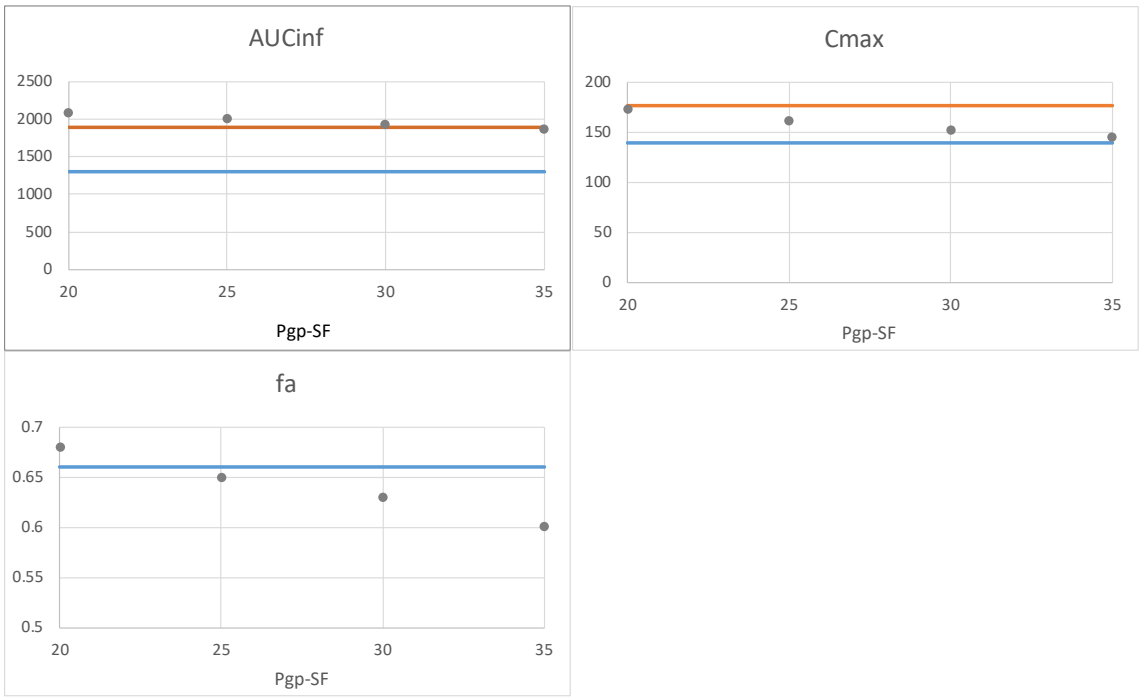


Observed data are indicated with red and blue lines and simulated data are indicated with grey circle. fa: fraction absorbed from gastrointestinal tract

(B)-1 Linear plot

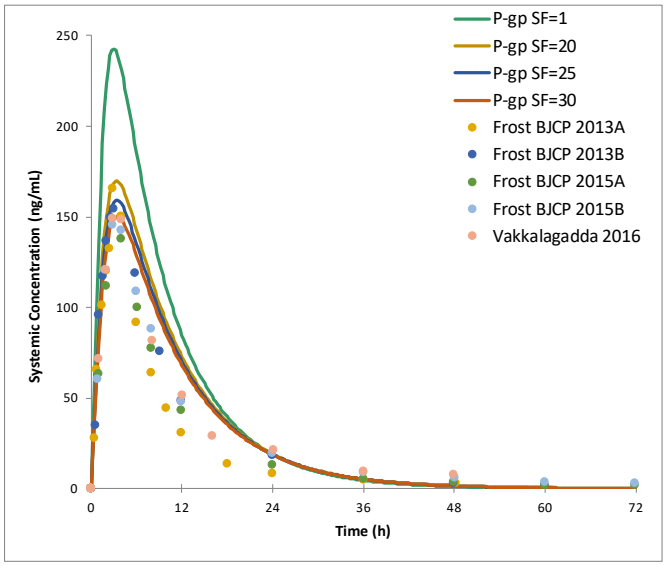


(B)-2 Semi-log plot

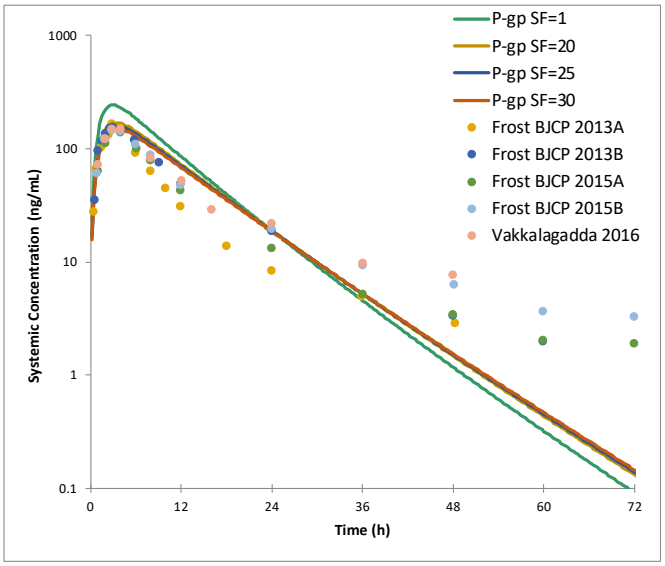


Lines are simulated plasma concentration profile and circles are observed plasma concentration of apixaban.

## Table S1-4 Input Parameters of the Apixaban PBPK Model

| Sample parameter | Value | Assumption(s) and references |
|---|---|---|
| **Physicochemical properties and blood binding** | | |
| Compound type | Neutral | 14 |
| Molecular weight | 459.5 | 9 |
| Log P | 1.65 | 14 |
| B/P ratio | 0.9 | 9 |
| $f_u$ | 0.1 | 9 |
| Plasma binding protein | HSA | 9 |
| **Absorption** | | |
| Absorption model | ADAM | |
| Formulation | Solution | Assumed because administration of oral tablet resulted in comparable exposure to that of oral solution administration[12] |
| $f_{u,Gut}$ | 0.158 | Predicted with Simcyp built-in module |
| $P_{app}$ ($10^{-6}$ cm/s)<br>LLC-PK1 cell passive permeability<br>Scalar | <br>6.0<br>1 | <br>13<br>Assumed |
| $P_{eff,man}$ ($10^{-4}$ cm/s) | 1.286 | Predicted |
| $P_{eff,man}$ ($10^{-4}$ cm/s) Ileum IV | 0.514 | Predicted (See details in the text) |
| $P_{eff,man}$ ($10^{-4}$ cm/s) Colon | 0.206 | Predicted (See details in the text) |
| **Distribution** | | |
| Distribution model | Full PBPK | |
| Prediction method of $V_{ss}$ | Method 2 | |
| $V_{ss}$ (L/kg) | 0.31 | Predicted |
| $K_p$ scalar | 1 | |
| **Elimination** | | |
| $CL_{iv}$ (L/h) | 3.3 | |
| $CL_R$ (L/h) | 1.0725 | Calculated from $CL_{iv}$ and elimination ratio of unchanged drug into urine |
| $CL_{add}$ (L/h) | 0.9735 | Calculated from $CL_{iv}$ and unrecovered ratio of dosed radioactivity |
| $CL_{int,\ CYP3A4}$ (mL/min/pmol)<br>$f_{u,mic}$ | 0.0112<br>1 | Retrograde calculation from $CL_{iv}$<br>Assumed |
| $CL_{int,HLM}$ (μL/min/mg protein)<br>$f_{u,inc}$ | 1.957<br>1 | Retrograde calculation from $CL_{iv}$<br>Assumed |
| **Transport** | | |
| $CL_{int,\ p\text{-}gp}$ in intestine (μL/min)<br>$f_{u,inc}$ | 1.39<br>1 | Estimated from *in vitro* P-gp facilitated transport velocity[13]<br>Assumed |
| RAF/REF for intestinal P-gp | 25 | Optimized in the current analysis. See text for the details. |

ADAM: advanced dissolution, absorption and metabolism, B/P ratio: blood to plasma concentration ratio, $CL_{add}$: additional systemic clearance, $CL_{int,CYP3A4}$: intrinsic clearance of CYP3A4 mediated metabolism, $CL_{int,HLM}$: intrinsic clearance in human liver microsome, $CL_{int,P\text{-}gp}$: intrinsic clearance of P-gp mediated transport, $CL_{iv}$: total systemic clearance after intravenous dosing, $CL_R$: renal clearance, $f_u$: fraction of unbound drug in plasma, $f_{u,Gut}$: fraction of unbound drug in enterocytes, $f_{u,inc}$: fraction of unbound drug in the *in vitro* incubation, $f_{u,mic}$: fraction of unbound drug in the *in vitro* microsomal incubation, HSA: human serum albumin, Log P: logarithm of the octanol–water partition coefficient, $P_{app}$: apparent passive permeability, $P_{eff,man}$: *in vivo* permeability, P-gp: P-glycoprotein, RAF/REF: relative activity factor/relative expression factor, $V_{ss}$: volume of distribution at steady-state

## S1.4 Apixaban PBPK Model Verification

At first, the developed po model was verified with multiple dose PK data after 2.5, 5, 10 and 25 mg bid and 10 and 25 mg qd. The results are shown in Table S1-5. The simulated plasma concentration profiles agreed with observed data at all dose levels and dosing regimen.

**Table S1-5 Observed and Predicted Pharmacokinetic Parameters of Apixaban after Single and Multiple Oral Administration of Apixaban at Several Dose Levels**

| | | Observed[4] | | Simulated‡ | |
|---|---|---|---|---|---|
| | | $AUC_{tau}$ (ng·h/mL) | $C_{max}$ (ng/mL) | $AUC_{tau}$ (ng·h/mL) | $C_{max}$ (ng/mL) |
| **2.5 mg bid** | **Day 1** | 353.3 (25) | 51.0 (27) | 314.7 (29) | 36.1 (31) |
| | **Day 7** | 462.8 (35) | 62.3 (37) | 487.0 (26) | 53.9 (26) |
| **5 mg bid** | **Day 1** | 600.6 (20) | 81.9 (18) | 628.8 (26) | 72.1 (28) |
| | **Day 7** | 1051.9 (9) | 128.5 (10) | 980.8 (24) | 108.5 (23) |
| **10 mg bid** | **Day 1** | 1608.3 (30) | 226.2 (38) | 1254.4 (27) | 143.9 (29) |
| | **Day 7** | 2424.9 (47) | 329.8 (45) | 1936.2 (24) | 214.6 (25) |
| **25 mg bid** | **Day 1** | 3108.6 (25) | 425.3 (24) | 3108.0 (28) | 356.9 (29) |
| | **Day 7** | 5850.3 (16) | 716.6 (21) | 4808.5 (25) | 533.3 (25) |
| **10 mg qd** | **Day 1** | 1589.6 (20) | 178.4 (19) | 1704.4 (27) | 141.8 (32) |
| | **Day 7** | 2015.7 (16) | 201.4 (15) | 1902.2 (27) | 158.0 (29) |
| **25 mg qd** | **Day 1** | 2868.1 (7) | 310.0 (12) | 4361.7 (27) | 361.0 (31) |
| | **Day 7** | 4248.3 (19) | 428.9 (20) | 4860.0 (26) | 401.3 (28) |

Geometric mean (CV%), bid: twice daily, qd: once daily

The apixaban model was verified with the DDI study results with ketoconazole, diltiazem, cyclosporin and rifampicin. The PBPK models for perpetrator drugs in the Simcyp compound library were used with modifications, as needed. The details of perpetrator drug models are described below:

Ketoconazole (Sim-Ketoconazole 400mg QD.cmpz), which is known as a strong CYP3A inhibitor and *in vitro* P-gp inhibitor[15], was used with adding a P-gp $K_i$ value. Based on the search in Drug Interaction Data Base (DIDB; University of Washington, Seattle, Washington, USA), ketoconazole's *in vitro* $IC_{50}$ value on P-gp is widely varying, ranging from 0.22 to 53.4 μM. The ketoconazole $K_i$ value for P-gp was investigated by Yamazaki *et al*. and the value of 0.2 μM resulted appropriate prediction of observed DDI with 500 mg bosutinib[16]. Furthermore, the clinical DDI study with digoxin[17] was used for verification of P-gp $K_i$ value and predicted $AUC_{24}$ without and with ketoconazole and $AUC_{24}$ ratio agreed with observed data (predicted/observed ratio of 1.1, 1.0 and 0.95, respectively). The ketoconazole model as a CYP3A inhibitor was verified by the software provider.

Diltiazem (Sim-Diltiazem.cmpz), which is known as a moderate CYP3A inhibitor[15], also inhibits P-gp. Although there are no *in vitro* P-gp inhibition data found in the literature, concomitant administration of diltiazem with digoxin increased digoxin $C_{max}$ and AUC 1.20- and 1.22-fold, respectively[18]. Diltiazem $K_i$ for P-gp was determined with sensitivity analysis to reproduce observed clinical DDI with digoxin and 0.1 μM agreed with the observed $C_{max}$ and AUC ratios (Figure S1-5). The clinical trials which

investigated diltiazem's P-gp inhibition effect are limited. One study showed that iv administration of digoxin after 14 days multiple oral administration of diltiazem had no effect on plasma exposure of digoxin[19] and the diltiazem model added with P-gp $K_i$ value determined in the present study reproduced the results. Diltiazem model as a CYP3A inhibitor was verified by the software provider. The desmethyl metabolite of diltiazem (Sim-Desmethyldiltiazem (MA).cmpz) also inhibits CYP3A and was used for DDI simulation.

**Figure S1-5 Sensitivity Analysis of Diltiazem $K_i$ of P-gp**

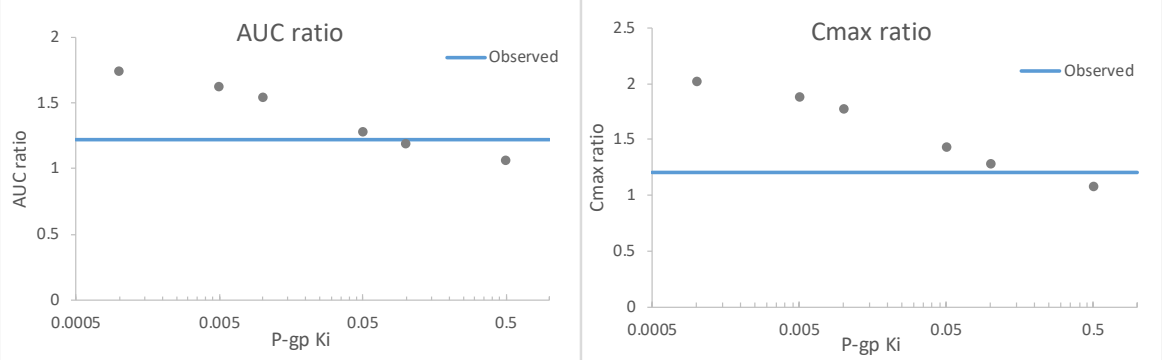


Blue line indicates the observed AUC and $C_{max}$ ratios and gray circles are predicted ACU and $C_{max}$ ratios

Cyclosporine (SV-Cyclosporine_Neoral.cmpz), which is known as a moderate CYP3A inhibitor and *in vitro* P-gp inhibitor[15] was used without any modifications to the software provided compound file. The cyclosporine model as a CYP3A inhibitor was verified by the software provider.

Rifampicin (SV-Rifampicin-MD.cmpz), which is known as a strong CYP3A inducer[15], also induces P-gp. Rifampicin is also reported to inhibit P-gp in *in vitro* studies. The details of P-gp induction and inhibition by rifampicin are described in the body text. The same assumptions of P-gp induction (3.5-fold and 2.0-fold increase in P-gp activity in intestine and liver, respectively) and P-gp inhibition ($K_i$ of 4.3 μM) were used throughout the present analysis. The rifampicin model as a CYP3A inducer was verified by the software provider.

The results of DDI verification of apixaban po model with several CYP3A4 and P-gp inhibitors/inducers are shown in Figure S1-6.

**Figure S1-6 Observed and Predicted Plasma Concentration-time Profile of Apixaban in Presence and Absence of CYP3A4 and P-gp Inhibitors/Inducer**

**(A) Ketoconazole**

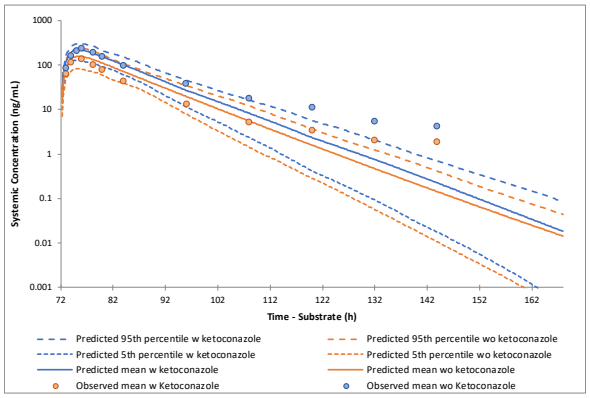


**(B) Diltiazem**

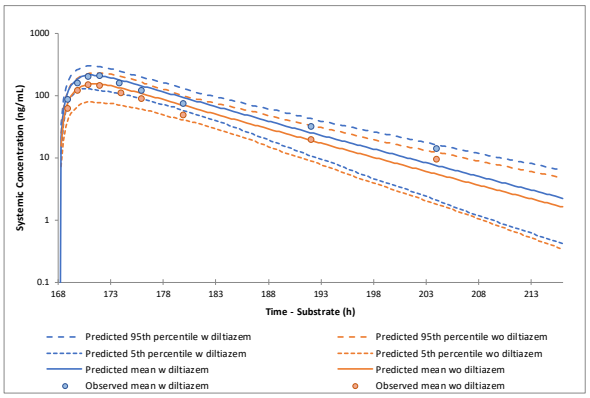


**(C) Cyclosporine**

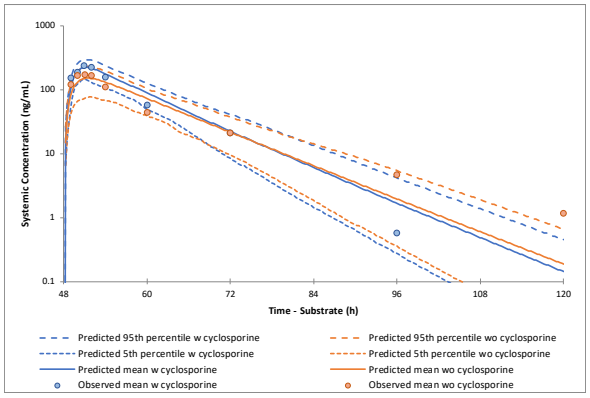


**(D) Rifampicin**

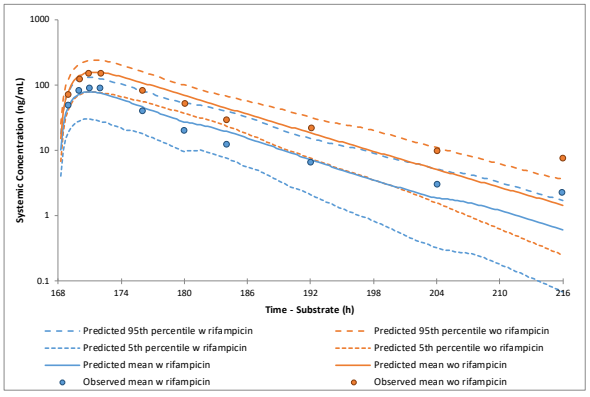


## S1.5 Reference


1 Vakkalagadda B. *et al*. Effect of rifampin on the pharmacokinetics of apixaban, an oral direct inhibitor of factor Xa. *Am. J. Cardiovasc. Drugs.* **16**, 119-127 (2016).

2 Frost C. *et al*. Apixaban, an oral, direct factor Xa inhibitor: single dose safety, pharmacokinetics, pharmacodynamics and food effect in healthy subjects. *Br. J. Clin. Parmacol*. **75**, 476-487 (2013a).

3 Frost C.E. *et al*. Effect of ketoconazole and diltiazem on the pharmacokinetics of apixaban, an oral direct factor Xa inhibitor. *Br. J. Clin. Pharmacol.* **79**, 838-846 (2015).

4 Frost C. *et al*. Safety, pharmacokinetics and pharmacodynamics of multiple oral doses of apixaban, a factor Xa inhibitor, in healthy subjects. *Br. J. Clin. Parmacol*. **76**, 776-786 (2013b).

5 Bashir B., Stickle D.F., Chervoneva I. & Kraft W.K. Drug-drug interaction study of apixaban with cyclosporine and tacrolimus in healthy volunteers. *Clin. Transl. Sci.* **11**, 590-596 (2018).

6 Raghavan N. *et al*. Apixaban metabolism and pharmacokinetics after oral administration to humans. *Drug Metab. Dispos.* **37**, 74-81 (2009).

7 Byon W., Nepal S., Schuster A.E., Shenker A. & Frost C.E. Regional gastrointestinal absorption of apixaban in healthy subjects. *J. Clin. Pharmacol.* **58**, 965-971 (2018).

8 ELIQUIS®: Clinical Pharmacology and Biopharmaceutics review(s). <https://www.accessdata.fda.gov/drugsatfda_docs/nda/2012/202155Orig1s000ClinPharmR.pdf> (2011). Accessed 17 July 2019.

9 Byon W., Garonzik S., Boyd R.A. & Frost C.E. Apixaban: A clinical pharmacokinetic and pharmacodynamic review. *Clin. Pharmacokinet.* **58**, 1265-1279 (2019).

10 Wang L. *et al*. *In vitro* assessment of metabolic drug-drug interaction potential of apixaban through cytochrome P450 phenotyping, inhibition, and induction studies. *Drug Metab. Dispos.* **38**, 448-458 (2010).

11 Rodgers T. & Rowland M. Mechanistic approaches to volume of distribution predictions: understanding the processes. *Pharm. Res.* **24**, 918-933 (2007).

12 Song Y. *et al*. Relative Bioavailability of apixaban solution or crushed tablet formulations administered by mouth or nasogastric tube in healthy subjects. *Clin. Ther.* **37**, 1703-1712 (2015).

13 Zhang D. *et al*. Characterization of efflux transporters involved in distribution and disposition of apixaban. *Drug Metab. Dispos*. **41**, 827-835 (2013).

14 Eliquis® Tablets. Interview Form (2017).

15 FDA Drug Development and Drug Interactions: Table of Substrates, Inhibitors and Inducers. <https://www.fda.gov/drugs/drug-interactions-labeling/drug-development-and-drug-interactions-table-substrates-inhibitors-and-inducers> (2020).

16 Yamazaki S., Loi C.M., Kimoto E., Costales C. & Varma M.V. Application of physiologically based pharmacokinetic modeling in understanding bosutinib drug-drug interactions: Importance of intestinal P-glycoprotein. *Drug Metab. Dispos.* **46**, 1200-1211 (2018).

17 Larsen U.L. *et al*. Human intestinal P-glycoprotein activity estimated by the model substrate digoxin. *Scand. J. Clin. Lab. Invest*. **67**, 123-134 (2007).

18 Rameis H., Magometschnigg D. & Ganzinger U. The diltiazem-digoxin interaction. *Clin. Pharmacol. Ther.* **36**, 183-189 (1984).

19 Jones W.N., Kern K.B., Rindone J.P., Mayersohn M., Bliss M. & Goldman S. Digoxin-diltiazem interaction: a pharmacokinetic evaluation. *Eur. J. Clin. Pharmacol.* **31**, 351-353 (1986).

## S2 Rivaroxaban PBPK Model Development and Verification as CYP3A4, P-gp and OAT3 Substrate

### S2.1 Objective

To develop and verify the PBPK model of rivaroxaban for its intended use in CYP3A and P-gp mediated drug-drug interaction simulations.

### S2.2 Summary

The PBPK models for rivaroxaban were previously investigated and reported in the literatures[1-6]. The purposes of the model development were different from each other and the models were only verified to fulfill their intended use. In the current analysis, the model was verified adequately to reproduce observed clinical DDI data which were related to the CYP3A and/or P-gp mediated elimination pathway of rivaroxaban. The literature data used in the current model development and verification are summarized in Table S2-1 and overall workflow is shown in Figure S2-1.

**Table S2-1 Summary of the Clinical Data Used in Rivaroxaban Model Development and Verification**

| Data category | Usage | Ref. |
|---|---|---|
| Mass Balance | Development | 7 |
| Single dose PK at 20 mg | Development | 8 |
| DDI with fluconazole | Development | 8 |
| Single dose PK at 10 mg | Verification | 8, 9 |
| Multiple dose PK | Verification | 10 |
| DDI with ketoconazole (200 mg) | Verification | 8 |
| DDI with ritonavir | Verification | 8 |
| DDI with clarithromycin | Verification | 8 |
| DDI with erythromycin | Verification | 8 |
| DDI with verapamil | Verification | 11 |

**Figure S2-1 Overall Workflow of Rivaroxaban PBPK Model Development and Verification**

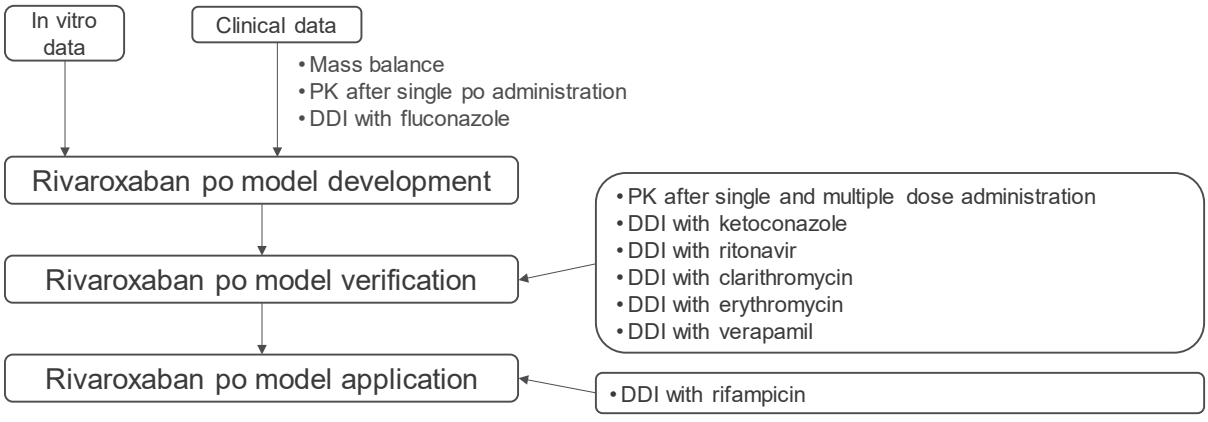

The absolute bioavailability of rivaroxaban was 66%[12] when 20 mg of rivaroxaban was administered at fasted condition. The area under the concentration-time curve (AUC) of rivaroxaban increased 39% after 20 mg dose administration with fed conditions, suggesting that incomplete absorption with fasting conditions was due to the dissolution step. The membrane permeability of rivaroxaban was investigated in an *in vitro* study and the apparent permeability ($P_{app}$) of rivaroxaban across LLC-PK1 cells in the presence of P-gp inhibitor, ivermectin, was $25.8\times10^{-6}$ cm/s[13]. Rivaroxaban was eliminated 65% into urine (36% as unchanged drug) and 24% into feces (7% as unchanged drug) after 10 mg of [$^{14}$C]rivaroxaban was orally administered[7]. In the hepatic metabolism, CYP3A, CYP2J2, and hydrolytic enzymes are considered to equally contribute[1]. Rivaroxaban is considered a substrate of P-gp and breast-cancer resistance protein (BCRP) *in vitro*. However, clinical data indicated that rivaroxaban is completely absorbed from the gut[12]. Furthermore, a clinical DDI study with verapamil, a moderate CYP3A inhibitor and P-gp inhibitor, rivaroxaban $C_{max}$ in plasma were not altered in presence of verapamil, indicating verapamil inhibition of gut P-gp did not affect rivaroxaban absorption[11]. Taken together, in the normal condition, P-gp is considered not to affect to rivaroxaban absorption from gut. The elimination pathway and mass balance are shown in Figure S2-2.

**Figure S2-2 Elimination Pathway and Mass Balance of Rivaroxaban (Final Model)**

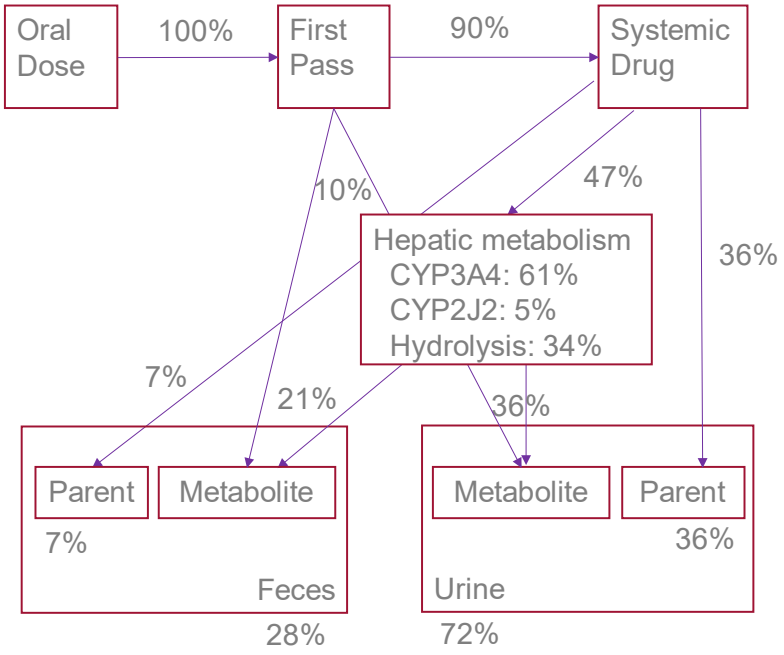


The rivaroxaban PBPK model was developed with an Advanced Dissolution, Absorption and Metabolism (ADAM) model and full PBPK accompanied by permeability limited liver model and mechanistic kidney model. The rivaroxaban PBPK model was first developed based on clinical PK data after 20 mg single dose administration at fed condition[8]. The contribution of CYP3A4 for hepatic metabolism was optimized using a clinical DDI study with fluconazole[8] since fluconazole only inhibits

CYP3A4 in the enzymes and transporters which are contributing to rivaroxaban absorption and elimination. The model was then verified with multiple dose PK data and clinical DDI study results with several CYP3A/P-gp inhibitors.

### A4.2 Rivaroxaban PBPK model development

Most of the parameters were referenced from the previously reported PBPK model by Cheong *et al*. except for ADAM parameters and contribution of CYP enzymes. Simcyp predicted effective permeability in the gut ($P_{eff,man}$) from a $P_{app}$ value of $25.8\times10^{-6}$ cm/s. The solid dosage formulation was selected and the aqueous phase intrinsic solubility and the aqueous buffer diffusion coefficients for uncharged active pharmaceutical ingredients monomer ($D_{uncharged}$) were optimized based on the dissolution profile in the literature[14]. The dissolution profile of rivaroxaban tablets in the media which was optimized to reproduce *in vivo* observed absorption profile that was extracted from the literature and the data was fitted to dissolution model in SIVA Toolkit version 3 (Certara UK Limited, Sheffield, UK). Aqueous phase intrinsic solubility and $D_{uncharged}$ were determined as 0.013 mg/mL and $7.5\times10^{-4}$ $cm^2$/min, respectively. When the reported P-gp kinetic parameter values ($J_{max}$: 37.83 pmol/min, $K_m$: 9.416 μM, RAF/REF: 1.5) were used[5], gut P-gp affected the absorption of rivaroxaban. Accordingly, the effect of gut P-gp was minimized by reducing the RAF/REF value 10-fold as determined by sensitivity analysis. This resulted in almost complete gut absorption of rivaroxaban. The model was then fitted to plasma-concentration time profile after 20 mg single dose administration at fed state[8] to optimize steady-state volume of distribution ($V_{ss}$) with adjusting $K_p$ scalar.

Intrinsic clearances of CYP3A4 and CYP2J2 were calculated from a retrograde model within the Simcyp simulator using an observed oral clearance ($CL_{po}$) of 11.3 L/h, renal clearance ($CL_r$) of 3.6 L/h[8], and additional systemic clearance of 1.24 L/h (calculated from $CL_{po}$ and unrecovered radioactivity of 11% as unknown systemic clearance). Biliary intrinsic clearance ($CL_{int}$ {Bile}) was also calculated from a retrograde model with canalicular efflux transporter clearance ($CL_{int,T,hP\text{-}gp}$). Passive diffusion clearance ($CL_{PD}$) in the sinusoidal membrane of the liver was set to 0.1 mL/min/million cells since the value was high enough to assume passive permeation of sinusoidal membrane was not a rate limiting step in hepatic elimination.

The parameters for kidney transporters (OAT3 and P-gp) and $CL_{PD}$ in basal and apical membrane of proximal tubular cells were referenced from the literature[5]. Cheong *et al*. calculated $CL_{PD,kidney}$ based on the scaling of *in vitro* determined passive permeability ($P_{pass}$) with nephron surface area, proximal tubular cells per gram of kidney (PTCPGK) and kidney weight. The calculated $CL_{PD,kidney}$ was $1.09\times10^{-5}$ mL/min/million cells. The observed and simulated plasma-concentration time profile of rivaroxaban are shown in Figure S2-3.

**Figure S2-3 Observed and Simulated Plasma Concentration Profile of Rivaroxaban after Single Oral Administration of Rivaroxaban at Fed State**

(A) Liner plot (B) Semi-log plot

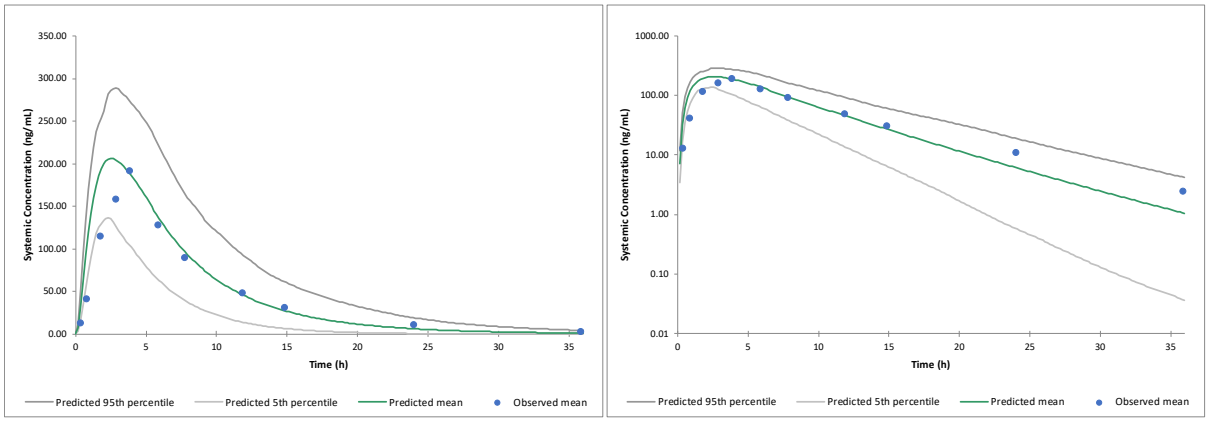


The initial model was then used for a DDI simulation with fluconazole. Fluconazole is reported not to inhibit CYP2J2[15], P-gp[16], and OAT3[17], and hence can be used for the estimation/verification of CYP3A4 contribution in hepatic metabolism of rivaroxaban. When using the initial assumptions of the contribution in metabolic pathways in the liver (CYP3A4: 37%, CYP2J2: 29%, hydrolysis: 34%)[5], the extent of DDI was underpredicted (Table S2-2). Then, the contribution of CYP3A4 and CYP2J2 metabolism was optimized to better reproduce clinical data. The contribution of hydrolysis was not changed since the metabolites produced by hydrolysis are clearly non-CYP metabolism and were quantitatively determined in clinical mass balance study[7]. As the result, 61% contribution of CYP3A4 and 5% contribution of CYP2J2 on oxidative metabolism of rivaroxaban reproduced the observed DDI results (Table S2-2). The conditions of retrograde calculation of $CL_{int,CYP3A4}$, $CL_{int,CYP2J2}$ and $CL_{int,Bile}$ are shown in Table S2-3. The parameters used for the final model are summarized in Table S2-4.

**Table S2-2 Observed and Predicted $AUC_{inf}$ and $C_{max}$ of Rivaroxaban in Absence and Presence of Fluconazole**

| | | Without fluconazole | | With fluconazole | | $AUC_{inf}$ ratio | $C_{max}$ ratio |
|---|---|---|---|---|---|---|---|
| | | $AUC_{inf}$ (ng·h/mL) | $C_{max}$ (ng/mL) | $AUC_{inf}$ (ng·h/mL) | $C_{max}$ (ng/mL) | | |
| **Initial** | **Observed[8]** | 1771 (887.4-2458) | 212.4 (83.03-318.2) | 2464 (1624-3612) | 268.8 (190.2-410.6) | 1.42 | 1.28 |
| | **Predicted** | 1660 (659.3-3332) | 207.2 (112.8-323.3) | 1970 (707.9-5087) | 221.1 (129.0-353.2) | 1.18 | 1.07 |
| | **P/O ratio** | 0.94 | 0.98 | 0.80 | 0.82 | 0.83 | 0.84 |
| **Optimized** | **Observed[8]** | 1771 (887.4-2458) | 212.4 (83.03-318.2) | 2464 (1624-3612) | 268.8 (190.2-410.6) | 1.42 | 1.28 |
| | **Predicted** | 1736 (695.5-3695) | 211.5 (101.9-326.3) | 2450 (979.7-5120) | 242.8 (127.6-369.9) | 1.41 | 1.15 |
| | **P/O ratio** | 0.98 | 1.00 | 0.99 | 0.90 | 0.99 | 0.90 |

AUC and $C_{max}$ values are shown as mean (range)

P/O ratio: Predicted/Observed ratio for mean values

## Table S2-3 Retrograde Calculation of Intrinsic Clearances of Rivaroxaban

| Parameters | Initial | Optimized |
|---|---|---|
| Population | Sim-Healthy Volunteers | Sim-Healthy Volunteers |
| Minimum Age (years) | 24 | 24 |
| Maximum Age (years) | 53 | 53 |
| Proportion of females | 0 | 0 |
| fa | 1 | 1 |
| fg | 0.9 | 0.9 |
| $fCL_{Bile}$(%) | 7 | 7 |
| $CL_{add}$ (L/h) | 1.243 | 0 |
| %HEPCL CYP3A4 | 37% | 61% |
| %HEPCL CYP2J2 | 29% | 5% |

fa: fraction absorbed from gut, fg: fraction escaping the metabolism in enterocyte, $fCL_{Bile}$: fraction of biliary clearance on overall clearance, $CL_{add}$: additional systemic clearance, %HEPCL: percentage in hepatic clearance

## Table S2-4 Input parameters of the rivaroxaban PBPK model

| Sample parameter | Value | Assumption(s) and references |
|---|---|---|
| **Physicochemical properties and blood binding** | | |
| Compound type | Neutral | 5 |
| Molecular weight | 435.88 | 5 |
| Log P | 1.5 | 5 |
| B/P ratio | 0.71 | 5 |
| $f_u$ | 0.065 | 5 |
| Plasma binding protein | HSA | 5 |
| **Absorption** | | |
| Absorption model | ADAM | |
| $f_{u,Gut}$ | 0.209 | Calculated with Simcyp built-in method |
| $P_{app}$ ($10^{-6}$ cm/s)<br>LLC-PK1 passive permeability<br>Scalar | <br>25.8<br>1 | <br>13<br>Assumed |
| $P_{eff,man}$ ($10^{-4}$ cm/s) | 3.184 | Calculated with Simcyp built-in method |
| Formulation | Solid formulation | |
| Intrinsic solubility (mg/mL) | 0.013 | Predicted with SIVA. See details in the text. |
| Uncharged diffusion coefficient ($10^{-4}$ $cm^2$/min) | 7.5 | Predicted with SIVA. See details in the text. |
| **Distribution** | | |
| Distribution model | Full PBPK | |
| Prediction method of $V_{ss}$ | Method 2 | |
| $V_{ss}$ (L/kg) | 0.577 | |
| $K_p$ scalar | 3.5 | Optimized with clinical data. See details in the text. |
| **Elimination** | | |
| $CL_{int,\ CYP3A4}$ (mL/min/pmol enzyme)<br>$f_{u,mic}$ | 0.127<br><br>1 | Calculated with Simcyp retro-grade model. See details in the text.<br>Assumed |
| $CL_{int,\ CYP2J2}$ (mL/min/pmol enzyme)<br>$f_{u,mic}$ | 2.264<br><br>1 | Calculated with Simcyp retro-grade model. See details in the text.<br>Assumed |
| $CL_{int,\ HLM}$ (mL/min/mg protein)<br>$f_{u,inc}$ | 8.943<br><br>1 | Calculated with Simcyp retro-grade model. See details in the text.<br>Assumed |
| **Transport** | | |
| $CL_{int,\ P\text{-}gp}$ in liver (µL/min/million hepatocytes)<br>$f_{u,inc}$ | 1.150<br><br>1 | Calculated with Simcyp retro-grade model as biliary clearance and applied to P-gp elimination on the canalicular membrane of hepatocytes<br>Assumed |
| $CL_{PD}$ in liver (mL/min/million hepatocetes) | 0.1 | High passive permeability was assumed on the sinusoidal membrane of hepatocytes considering rivaroxaban is a highly permeable compound. |
| $CL_{int,\ OAT3}$ in kidney (µL/min/million PT cells)<br>$f_{u,Kidney\ cell}$ | 43<br><br>0.3788975 | 5<br><br>5 |
| $J_{max,\ P\text{-}gp}$ in kidney (pmol/min/million PT cells) | 80.921 | 5 |
| $K_{m,\ P\text{-}gp}$ in kidney (µM) | 9.416 | 5 |
| RAF/REF for P-gp in kidney | 4 | 5 |
| $CL_{PD}$ in kidney (mL/min/million PT cells) | 0.0000109 (Model 1)<br>0.1 (Model 2) | 5<br>Assumed |
| $J_{max,\ P\text{-}gp}$ in intestine (pmol/min) | 37.830 | 5 |
| $K_{m,\ P\text{-}gp}$ in intestine (µM)<br>$f_{u,inc}$ | 9.416<br>1 | 5<br>Assumed |
| A ($cm^2$) | 0.33 | 5 |
| RAF/REF for P-gp in intestine | 0.15 | Optimized. See details in the text. |

A: insert growth area of the transwell, ADAM: advanced dissolution, absorption and metabolism, B/P ratio: blood to plasma concentration ratio, $CL_{add}$: additional systemic clearance, $CL_{int,CYP2J2}$: intrinsic clearance of CYP2J2 mediated metabolism, $CL_{int,CYP3A4}$: intrinsic clearance of CYP3A4 mediated metabolism, $CL_{int, HLM}$: intrinsic clearance in liver microsome, $CL_{int, OAT3}$: intrinsic clearance of OAT3 mediated transport, $CL_{int,P\text{-}gp}$: intrinsic clearance of P-gp mediated transport, $CL_{iv}$: total systemic clearance after intravenous dosing, $CL_{PD}$: passive diffusion clearance, $CL_R$: renal clearance, $f_u$: fraction of unbound in plasma, $f_{u,Gut}$: fraction of unbound in enterocytes, $f_{u,inc}$: fraction of unbound drug in the *in vitro* incubation, $f_{u,Kidney\ cell}$: fraction of unbound drug in kidney cell, $f_{u,mic}$: fraction of unbound drug in the *in vitro* microsomal incubation, HSA: human serum albumin, $J_{max,P\text{-}gp}$: maximum rate of P-gp mediated transport, $K_{m,P\text{-}gp}$: Michaelis constant of P-gp mediated transport, Log P: logarithm of the octanol–water partition coefficient, $P_{app}$: apparent passive permeability, $P_{eff,man}$: *in vivo* permeability, P-gp: P-glycoprotein, RAF/REF: relative activity factor/relative expression factor, $V_{ss}$: volume of distribution at steady-state

## S2.3 Rivaroxaban PBPK model verification

At first, the predictability of PK after 10 mg single oral dose administration and 5, 10, 20, and 30 mg multiple oral dose administrations was tested and compared with clinical data. The results are shown in Table S2-5.

**Table S2-5 Observed and Predicted $C_{max}$ and AUC of Rivaroxaban after 10 mg Single Oral Dose and 5, 10, 20 and 30 mg Multiple Oral Dose Administrations of Rivaroxaban**

A) Single dose

| | | **$AUC_{inf}$ (ng·h/mL)** | **$C_{max}$ (ng/mL)** |
|---|---|---|---|
| **Predicted** | **trial 1** | 1108 | 134.1 |
| | **trial 2** | 1219 | 134.0 |
| | **trial 3** | 1049 | 124.0 |
| | **trial 4** | 1098 | 131.7 |
| | **trial 5** | 1027 | 132.9 |
| | **trial 6** | 953 | 127.1 |
| | **trial 7** | 1086 | 131.4 |
| | **trial 8** | 1074 | 128.5 |
| | **trial 9** | 1111 | 129.3 |
| | **trial 10** | 946 | 118.8 |
| | **mean** | 1067 | 129.2 |
| **Observed** | **study 1**[8] | 892 | 138.1 |
| | **study 2**[8] | 1000 | 153.7 |
| | **study 3**[8] | 964 | 139.4 |
| | **study 4**[8] | 1069 | 170.5 |
| | **study 5**[9] | 1024 | 125 |
| | **mean** | 990 | 145 |
| **Predicted/observed ratio** | | 1.08 | 0.889 |

B) Multiple dose

| | | Observed[10] | | Simulated (Model 1) | | Simulated (Model 2) | |
|---|---|---|---|---|---|---|---|
| | | **$AUC_{tau}$ (μg·h/L)** | **$C_{max}$ (μg/L)** | **$AUC_{tau}$ (μg·h/L)** | **$C_{max}$ (μg/L)** | **$AUC_{tau}$ (μg·h/L)** | **$C_{max}$ (μg/L)** |
| **5 mg bid** | **Day 7** | 458.5 (13.1) | 85.3 (17.7) | 484.2 (33) | 73.5 (22) | 517.7 (30) | 76.8 (21) |
| **10 mg bid** | **Day 7** | 863.8 (18.6) | 158.0 (18.8) | 962.9 (33) | 143.6 (23) | 1023.1 (30) | 149.7 (22) |
| **20 mg bid** | **Day 7** | 1903.0 (24.5) | 318.1 (18.7) | 1838.0 (33) | 257.0 (25) | 1944.2 (31) | 267.9 (24) |
| **30 mg bid** | **Day 7** | 2728.0 (14.6) | 451.9 (10.5) | 2443.7 (34) | 327.2 (26) | 2595.3 (33) | 342.0 (26) |

Geometric mean (CV%)

Next, the predictability of a DDI study when rivaroxaban was concomitantly administered with ketoconazole, ritonavir, clarithromycin, erythromycin, verapamil, and rifampicin were investigated. The software vendor provided compound files for the perpetrator drugs were used with modification, as needed.

Ketoconazole is reported to inhibit CYP2J2[5] and OAT3[18] in *in vitro* studies. The *in vitro* reported $K_i$ value for CYP2J2 (0.082 μM) was used without modification. $K_i$ value for OAT3 was optimized by Cheong *et al*. to reproduce clinically observed DDI results of rivaroxaban when 400 mg ketoconazole was concomitantly administered. In the present analysis, the optimized value of 0.01 μM was used and the DDI was simulated for rivaroxaban vs 200 mg ketoconazole for the purpose of verification.

Ritonavir (SV-Ritonavir.cmpz), which is reported to inhibits and induces CYP3A[19] also inhibits CYP2J2[20] and OAT3[17]. The *in vitro* reported $IC_{50}$ value for CYP2J2 was used after dividing by two (0.49 μM). As for OAT3 $K_i$, at first the *in vitro* reported $IC_{50}$ value divided by two (2.35 μM) was used but the DDI simulation results with rivaroxaban were not well reproduced. Then, a 100-fold lower value was used since, in the ketoconazole OAT3 inhibition, an approximately 100-fold difference was observed between *in vitro* $K_i$ value and *in vivo* $K_i$ value (0.86~15.77 μM[5] and 0.01 μM, respectively). Ritonavir also inhibits P-gp and the optimization of P-gp $K_i$ and verification was done by the software vendor.

Clarithromycin (SV-Clarithromycin.cmpz), which is known as a strong CYP3A inhibitor[21], also inhibits P-gp *in vitro*[18]. As *in vitro* reported $IC_{50}$ value resulted in underestimation of clinical DDI study result with digoxin, the $K_i$ value was optimized and verified. A summary of P-gp $K_i$ optimization and verification is shown in Table S2-6.

**Table S2-6 Optimization and Verification of P-gp $K_i$ of Clarithromycin using Clinical DDI Study Results with Digoxin**

| Purposes | P-gp $K_i$ (μM) | Observed | | Predicted | |
|---|---|---|---|---|---|
| | | AUC ratio | $C_{max}$ ratio | AUC ratio | $C_{max}$ ratio |
| Optimization[22] | 0.4 | 1.64 | 1.83 | 1.16 | 1.20 |
| | 0.1 | 1.64 | 1.83 | 1.25 | 1.33 |
| | 0.04 | 1.64 | 1.83 | 1.34 | 1.42 |
| | 0.01 | 1.64 | 1.83 | 1.35 | 1.46 |
| Verification[22] | 0.04 | 1.19 | ND | 1.16 | ND |
| Verification[23] | 0.04 | 1.47 | 1.75 | 1.36 | 1.46 |

ND: not determined

*In vitro* investigations on whether clarithromycin inhibits CYP2J2 were not found within the public space; therefore, it was assumed that clarithromycin does not inhibit CYP2J2. Furthermore, clarithromycin did not inhibit OAT3 in an *in vitro* study[24]. The model verification of CYP3A inhibition was done by the software vendor.

Erythromycin (Sim-Erythromycin.cmpz), which is known as a moderate CYP3A inhibitor[21], also inhibits P-gp[1]. The reported $K_i$ value of 11 μM was used without modification. A clinical DDI study reported no effect of erythromycin on digoxin exposure[25]. In the present analysis, it was confirmed that modified erythromycin model (addition of P-gp $K_i$) did not affect P-gp exposure (data not shown). Erythromycin is reported not to inhibit CYP2J2[15] and OAT3[26]. The model verification of CYP3A inhibition was done by the software vendor.

Verapamil (SV-Verapamil.cmpz), which is known as a moderate CYP3A inhibitor and P-gp inhibitor[21], also inhibits CYP2J2[5]. The reported $K_i$ values for verapamil and its major metabolite, norverapamil (12.2 and 162 μM, respectively), were used without modifications. Verapamil and norverapamil did not inhibit OAT3 in an *in vitro* study[5]. The model verification of CYP3A and P-gp inhibition were done by software vendor.

Rifampicin is reported to inhibit OAT3[24] but not to inhibit or induce CYP2J2[27]. The *in vitro* reported $IC_{50}$ value for OAT3 was used after dividing by two. As for P-gp induction, details are described in body text.

Although the verification of CYP2J2 inhibition by ketoconazole, ritonavir, and verapamil were not shown because of the lack of the clinical DDI results, the impact of CYP2J2 inhibition is considered not large since the contribution of CYP2J2 on elimination of rivaroxaban is low as discussed in the body text. The results of DDI simulations when rivaroxaban is concomitantly administered with ketoconazole, ritonavir, clarithromycin, erythromycin, verapamil and rifampicin were summarized in Table 3. The observed and predicted plasma concentration-time profiles of rivaroxaban in presence and absence of ritonavir, clarithromycin, erythromycin and verapamil are shown in Figure S2-5

**Figure S2-4 Observed and Predicted Plasma Concentration-time Profile of Rivaroxaban in Presence and Absence of CYP3A4 and P-gp Inhibitors**

**(A) Ritonavir**

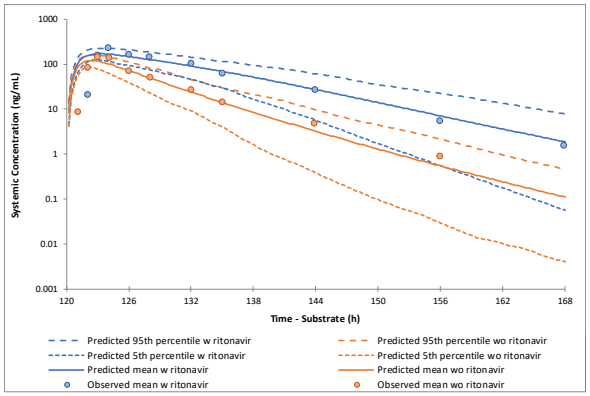


**(B) Clarithromycin**

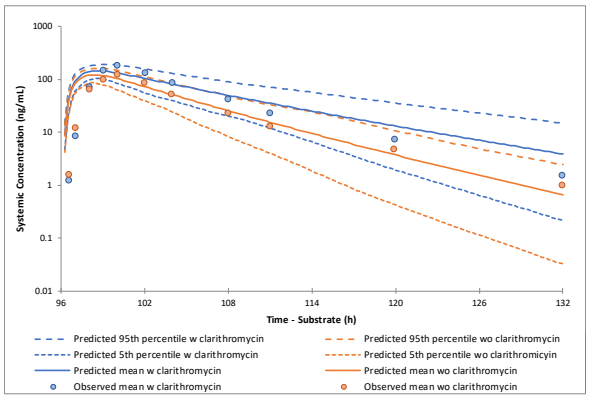


**(C) Erythromycin**

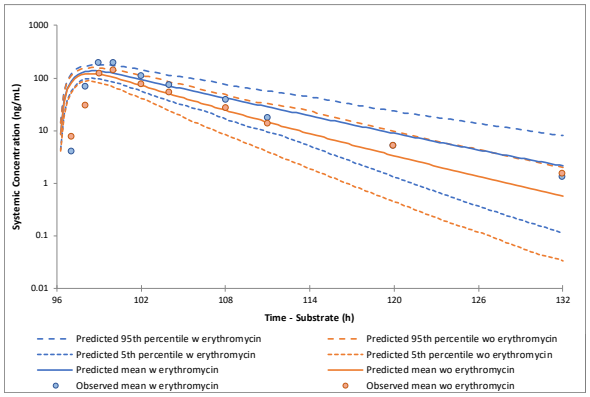


**(D) Verapamil**

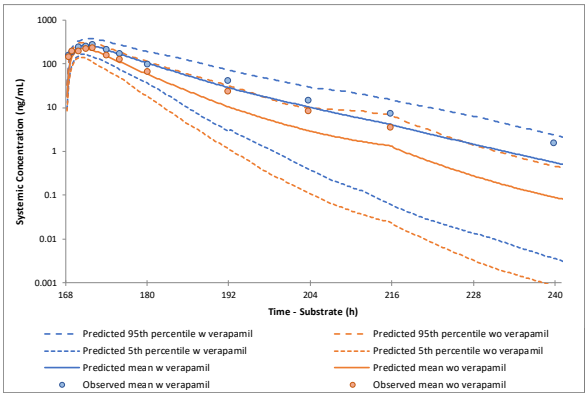


## A4.4 References


1 Grillo JA. *et al*. Utility of a physiologically-based pharmacokinetic (PBPK) modeling approach to quantitatively predict a complex drug-drug-disease interaction scenario for rivaroxaban during the drug review process: implications for clinical practice. *Biopharm. Drug Dispos.* **33**, 99-110 (2012).

2 Ismail M., Lee V.H., Chow C.R. & Rubino C.M. Minimal physiologically based pharmacokinetic and drug-drug-disease interaction model of rivaroxaban and verapamil in healthy and renally impaired subjects. *J. Clin. Pharmacol.* **58**, 541-548 (2018).

3 Willmann S. *et al*. Pharmacokinetics of rivaroxaban in children using physiologically based and population pharmacokinetic modelling: an EINSTEIN-Jr phase I study. *Thromb. J.* **16**, 32 (2018).

4 Xu R., Ge W. & Jiang Q. Application of physiologically based pharmacokinetic modeling to the prediction of drug-drug and drug-disease interactions for rivaroxaban. *Eur. J. Clin. Pharmacol.* **74**, 755-765 (2018).

5 Cheong E.J.Y., Teo D.W.X., Chua D.X.Y. & Chan E.C.Y. Systematic development and verification of a physiologically-based pharmacokinetic model of rivaroxaban. *Drug Metab. Dispos.* **47**, 1291-1306 (2019).

6 Stader F., Kinvig H., Penny M.A., Battegay M., Siccardi M. & Marzolini C. Physiologically based pharmacokinetic modelling to identify pharmacokinetic parameters driving drug exposure changes in the elderly. *Clin. Pharmacokinet.* **59**, 383-401 (2019).

7 Weinz C., Schwarz T., Kubitza D., Mueck W. & Lang D. Metabolism and excretion of rivaroxaban, an oral, direct factor Xa inhibitor, in rats, dogs, and humans. *Drug Metab. Dispos.* **37**, 1056-1064 (2009).

8 Mueck W., Kubitza D. & Becka M. Co-administration of rivaroxaban with drugs that share its elimination pathways: pharmacokinetic effects in healthy subjects. *Br. J. Clin. Pharmacol.* **76**, 455-466 (2013).

9 Kubitza D., Becka M., Schwers S. & Voith B. Investigation of pharmacodynamic and pharmacokinetic interactions between rivaroxaban and enoxaparin in healthy male subjects. *Clin. Pharmacol. Drug Dev*. **2**, 270-277 (2013).

10 Kubitza D., Becka M., Wensing G., Voith B. & Zuehlsdorf M. Safety, pharmacodynamics, and pharmacokinetics of BAY 59-7939--an oral, direct Factor Xa inhibitor--after multiple dosing in healthy male subjects. *Eur. J. Clin. Pharmacol.* **61**, 873-880 (2005).

11 Greenblatt D.J., Patel M., Harmatz J.S., Nicholson W.T., Rubino C.M. & Chow C.R. Impaired rivaroxaban clearance in mild renal insufficiency with verapamil coadministration: Potential implications for bleeding risk and dose selection. *J. Clin. Pharmacol.* **58**, 533-540 (2018).

12 XARELTO®: Clinical Pharmacology and Biopharmaceutics Review(s). <https://www.accessdata.fda.gov/drugsatfda_docs/nda/2011/202439Orig1s000ClinPharmR.pdf> (2011). Accessed 27 April 2020.

13 Gnoth M.J., Buetehorn U., Muenster U., Schwarz T. & Sandmann S. *In vitro* and *in vivo* P-glycoprotein transport characteristics of rivaroxaban. *J. Pharmacol. Exp. Ther*. **338**, 372-380 (2011).

14 Wingert N.R., Dos Santos N.O., Campanharo S.C., Simon E.S., Volpato N.M. & Steppe M. *In vitro* dissolution method fitted to *in vivo* absorption profile of rivaroxaban immediate-release tablets applying *in silico* data. *Drug Dev. Ind. Pharm.* **44**, 723-728 (2018).

15 Lee C.A. *et al*. Identifying a selective substrate and inhibitor pair for the evaluation of CYP2J2 activity. *Drug Metab. Dispos*. **40**, 943-951 (2012).

16 Wang E.J., Lew K., Casciano C.N., Clement R.P. & Johnson W.W. Interaction of common azole antifungals with P glycoprotein. *Antimicrob. Agents Chemother*. **46**, 160-165 (2002).

17 Yoshida K., Maeda K. & Sugiyama Y. Transporter-mediated drug--drug interactions involving OATP substrates: predictions based on *in vitro* inhibition studies. *Clin. Pharmacol. Ther*. **91**, 1053-1064 (2012).

18 Vermeer L.M., Isringhausen C.D., Ogilvie B.W. & Buckley D.B. Evaluation of ketoconazole and its alternative clinical CYP3A4/5 inhibitors as inhibitors of drug transporters: The *in vitro* effects of ketoconazole, ritonavir, clarithromycin, and itraconazole on 13 clinically-relevant drug transporters. *Drug Metab. Dispos*. **44**, 453-459 (2016).

19 Umehara K.I., Huth F., Won C.S., Heimbach T. & He H. Verification of a physiologically-based pharmacokinetic model of ritonavir to estimate drug-drug interaction potential of CYP3A4 substrates. *Biopharm. Drug Dispos.* **39**, 152-163 (2018).

20 Kaspera R. *et al*. Investigating the contribution of CYP2J2 to ritonavir metabolism *in vitro* and *in vivo*. *Biochem. Pharmacol*. **91**, 109-118 (2014).

21 FDA Drug Development and Drug Interactions: Table of Substrates, Inhibitors and Inducers. <https://www.fda.gov/drugs/drug-interactions-labeling/drug-development-and-drug-interactions-table-substrates-inhibitors-and-inducers> (2020).

22 Rengelshausen J. *et al*. Contribution of increased oral bioavailability and reduced nonglomerular renal clearance of digoxin to the digoxin-clarithromycin interaction. *Br. J. Clin. Pharmacol*. **56**, 32-38 (2003).

23 Gurley B.J., Swain A., Williams D.K., Barone G. & Battu S.K. Gauging the clinical significance of P-glycoprotein-mediated herb-drug interactions: comparative effects of St. John's wort, Echinacea, clarithromycin, and rifampin on digoxin pharmacokinetics. *Mol. Nutr. Food Res.* **52**, 772-779 (2008).

24 Parvez MM, Kaisar N, Shin HJ, Jung JA, Shin J-G. Inhibitory Interaction Potential of 22 Antituberculosis Drugs on Organic Anion and Cation Transporters of the SLC22A Family. Antimicrob Agents Chemother. 2016;60(11):6558-67.

25 Tsutsumi K. *et al*. The effect of erythromycin and clarithromycin on the pharmacokinetics of intravenous digoxin in healthy volunteers. *J. Clin. Pharmacol*. **42**, 1159-1164 (2002).

26 Lu X. *et al*. The inhibitory effects of eighteen front-line antibiotics on the substrate uptake mediated by human organic anion/cation transporters, organic anion transporting polypeptides and oligopeptide transporters in *in vitro* models. *Eur. J. Pharm. Sci.* **115**, 132-143 (2018).

27 Evangelista E.A., Kaspera R., Mokadam N.A., Jones J.P., 3rd & Totah R.A. Activity, inhibition, and induction of cytochrome P450 2J2 in adult human primary cardiomyocytes. *Drug Metab. Dispos.* **41**, 2087-2094 (2013).